ASTRONOMY & ASTROPHYSICS
SUPPLEMENT SERIES

MAY 1987, PAGE 263

Astron. Astrophys. Suppl. Ser. **69,** 263-279 (1987)

HI observations of lenticular and early type galaxies (*)

P. Chamaraux ([1]), C. Balkowski ([2]) and P. Fontanelli ([2])

([1]) UA 324, DERADN, Observatoire de Paris, Section de Meudon, 92195 Meudon Principal Cedex, France
([2]) UA 173, Université Paris VII, D.A.E.C., Observatoire de Paris, Section de Meudon, 92195 Meudon Principal Cedex, France

Received May 29, accepted October 28, 1986

Summary. — We present high sensitivity HI observations of 56 galaxies, mostly S0's (47 objets), carried out with the Arecibo radiotelescope. Twelve S0's and four S0/a spirals have been detected, among which 12 for the first time, and 9 of them have been mapped. In addition, absorption lines have been found in two S0's. A detailed discussion of the results of the mapping has allowed to solve several cases of confusion and to find out two possible cases of HI ring structures or flat rotation curves in S0's. Finally for 6 mapped galaxies, a simple deconvolution procedure has led to the derivation of the total HI fluxes and of the HI diameters ; on the average, the ratio of the HI diameter to the optical one is found to be 30 % higher for the S0's than for the spirals.

Key words : lenticular galaxies — radio lines : 21 cm.

1. Introduction.

The question of the origin of the S0 galaxies is still a matter of discussion : do they originate from ancient spirals having lost their gas, or have they been formed originally as S0's or can they have the one or the other origin, depending on their environment for instance ? The study of the HI content of these galaxies is certainly an important step to solve this problem, since it can show the relationship of the S0's to the spirals and shed light on possible environmental effects.

Several HI surveys of S0's have been carried out ; the most extensive one has been performed at Arecibo by Giovanardi *et al.* (1983) on 145 S0's and early spirals, with a detection rate of about 25 % for the S0's. The purpose of our observations was to complete the previous S0 surveys in order to obtain a complete sample of S0's down to an apparent diameter of 2' observed with the high sensitivity of the Arecibo telescope. The study of the true distribution of the HI contents of the S0's of that complete sample (taking into account the upper limits of detection) and of the influence of the environment on these contents is presented in another paper (Chamaraux *et al.*, 1986).

The structure of the present paper is the following : the sample, the observations and the HI profile parameters are presented in section 2. In section 3, we discuss individual objects, in particular cases of possible confusion. Section 4 is devoted to the computation of the HI diameters and of the total HI fluxes for 6 mapped galaxies. A summary of the most salient results is given in section 5.

2. The sample, the observations and the HI profile parameters.

2.1 THE SAMPLE. — As it has been shown by Chamaraux *et al.* (1986), the best parameter characterizing the HI content of S0 galaxies is, as for the spirals, the HI mean surface density σ_H defined by :

$$\sigma_H = M_H/(\pi A_0^2/4),$$

where M_H is the HI mass of the galaxy and A_0 its linear diameter ; this parameter can also be written as a function of the observable quantities :

$$\sigma_H = 0.74\, F_H/a_0^2\,, \qquad (1)$$

(*) Observations carried out with the Arecibo radiotelescope. The National Astronomy and Ionosphere Center is operated by Cornell University under contract with the National Science Foundation.

Send offprint requests to : P. Chamaraux.

where F_H is the HI flux of the galaxy in Jy km s^{-1} and a_0 its apparent diameter in arcmin, σ_H being expressed in 10^{-3} g cm^{-2}. In all the following, we shall use for a_0, as usual, the apparent major diameter to the brightness level 25 m/□″, corrected to face-on view and for galactic extinction according to de Vaucouleurs *et al.* (1976, hereafter RC2). The region where it is important to know better the σ_H-distribution is of course the zone of small σ_H-values, where there are few detections, namely the zone $\sigma_H < 0.2 \times 10^{-3}$ g cm^{-2}. Since the limit of HI flux reached at Arecibo is about 0.5 Jy km s^{-1}, (1) shows that the study of this zone can only be done by observations of S0's having apparent diameter larger than 2′. Hence our purpose was to observe the remaining such objects no yet observed at Arecibo in order to have high sensitivity HI observations for all the S0's having $a_0 \geqslant 2'$.

Therefore our observed sample comprises basically 40 S0 galaxies, i.e. having a type $T = -1$, -2 or -3 in RC2, an RC2 apparent diameter larger than 2 arcmin, located in the declination range accessible to the Arecibo radiotelescope ($-1° \leqslant \delta \leqslant +38°$), and still not observed at Arecibo, or observed but not mapped for the largest ones.

In addition, a few early spirals have been observed to study the transition between S0's and spirals, and a few S0's with $a_0 < 2.0'$ as well in the zones of right ascensions relatively empty of larger S0's.

A total of 56 galaxies has thus been observed ; the obviously confused objects have been generally rejected from the sample.

With the completion of our survey, of the 118 RC2 S0's having apparent diameters larger than 2 arcmin and $-1° \leqslant \delta \leqslant 38°$, only 14 have not been observed at Arecibo, among which only 5 are not confused, leading to a completeness of 88 %. On the other hand, the number $N(\geqslant a)$ of RC2 S0's having an apparent diameter larger than a varies as a^{-3} down to 2′ (Fig. 1), indicating that the RC2 is substantially complete to that limit of diameter.

2.2 THE OBSERVATIONS. — All the 21-cm line observations described in this paper were carried out with the Arecibo 305 m radiotelescope in two runs during May 1982 and July 1983. Most of the data were taken with the 14 m dual polarization feed, HPBW = 3.2 arcmin, simultaneously collecting two independent circularly polarized components of the incoming signal ; only in 10 cases (see Tab. I), the one polarization flat feed (HPBW = 3.9′) was chosen due to its lower sidelobes contribution, but for all the other objects the dual polarization circular feed was used because its system temperature ($\simeq$ 45-60 K) is lower than that of the flat feed ($\sim$ 70-90 K) and therefore its sensitivity is higher. Pointing uncertainties are about 20″ (Hewitt *et al.*, 1983), which is small compared to the beam size.

The spectral characteristics of the signal were analysed into a 1008 channels autocorrelation spectrometer operating in a four quadrants mode of 252 channels each. The four quadrants were covering the same frequency range of 10 MHz centred at the redshift of the observed galaxy corresponding to a velocity range of 2111 km s^{-1} for an object at rest, and resulting in a velocity resolution of 8.4 km s^{-1}. The observations were carried out in a total power mode in which 5 min long ON-source scans were followed by OFF-source scans of the same duration and in the same telescope configuration as the ON. Thus, the OFF positions were always at more than 1° from the ON, i.e. well beyond the edge of the galaxy observed, eliminating any risk of confusion between ON and OFF. Corrections for zenith angle and frequency dependence were applied to all spectra. Calibrations for the flux density scale were frequently obtained in the course of the observing runs using continuum sources from the catalog of Bridle *et al.* (1972).

The program galaxies were observed at the coordinates corresponding to the average of the accurate positions given by Dressel and Condon (1976) on one hand, and Gallouët and Heidmann (1971) or Gallouët *et al.* (1973) on the other hand, or at the position given by one of the catalogues if not available in both, or directly measured on the PSS prints otherwise. In addition, 12 objects, giving a strong signal when pointing at their central position, were observed at several positions along their major axis. Other 9 galaxies were also observed at one beam off centre along their main axis, although not detected at their central position. Indeed detailed mapping carried out at Westerbork (van Woerden *et al.*, 1983) has shown that in several S0's, the HI is mainly concentrated in clouds or ring features located sometimes outside the optical limits. If some program galaxies have such distribution with an HI ring larger than the 3.2′ Arecibo HPBW, it can well happen that no signal is detected at the central position, whereas something is observed one beam off, hence our observing procedure. In fact, we have not found such a peculiar situation in the 9 objects so observed.

2.3 THE HI PROFILE PARAMETERS. — The profiles of the detected galaxies are shown in figure 2 after convolution with a rectangular function 3 channels wide and with an Hanning cosine function and after removal of a 3rd degree or less polynomial baseline. The velocity scale is heliocentric. The number in the upper left corner of each profile represents the whole flux density range of the figure in mJy.

Table I contains the 21-cm line parameters for all the observed galaxies ; uncertain parameters corresponding to possibly confused objects are in parentheses ; the entries are as follows :

Column 1 : Name of the galaxy : N for NGC, I for IC, U for UGC ; a letter c indicates a confusing object found in a mapping.

Column 2 : Position angle from UGC, for the mapped galaxies only.

Column 3 : Distance of the observed position from the centre of the galaxy, in arcmin. When along the main axis, the positions are preceded by E or W according to wether they correspond to easterly or westerly locations with respect to the galaxy centre ; when along the minor axis, the positions are preceded by e and w with similar conventions. N designates a point exactly at the North of the galaxy centre. When no position angle is available (galaxy almost face-on), E and W are exactly east and west of the galaxy centre, as if the position angle were 90°.

Column 4 : Morphological type from RC2 if available or from UGC otherwise.

Column 5 : RC2 apparent major diameter in arcmin corrected to face-on view and for galactic extinction ; diameters not available in the RC2 have been reduced to the D_{25} system and corrected following the RC2 precepts.

Column 6 : Heliocentric optical velocity in km s^{-1} from the CfA redshifts survey (Huchra *et al.*, 1983) if available, or from RC2 otherwise.

Column 7 : Heliocentric radial velocity in km s^{-1} defined as the midpoint of the 20 % level of the peak flux of our 21-cm line profile. The quoted uncertainty is computed from the signal-to-noise ratio using the formula given by Bicay and Giovanelli (1986) (hereafter B.G.). As in the three following columns, the underlined values correspond to parameters corrected for confusing galaxies (see Sect. 3) ; the associated uncertainties are given in parentheses : they represent in fact lower limits since they don't account for the uncertainty introduced by the correction for confusion.

Column 8 : HI profile width in km s^{-1} measured at 20 % of the peak flux, with its associated uncertainty computed according to B.G. The correction of the width for the 8.4 km s^{-1} instrumental velocity resolution computed according to Fisher and Tully's (1981) formula is lower than 1 km s^{-1}, and has therefore been neglected.

Column 9 : HI profile width in km s^{-1} measured at 50 % of the peak flux, with its associated uncertainty computed according to B.G., instrumental correction negligible.

Column 10 : HI flux expressed in Jy km s^{-1} with its associated uncertainty computed according to B.G. In case of non-detections, the upper limits have been calculated using $F_H = 3 \times \sigma \times 300$ Jy km s^{-1}, where σ is the r.m.s. noise in the baseline. Observations carried out with the flat feed are denoted with an asterisk.

Column 11 : An asterisk indicates objects discussed in details in section 3 ; the total HI flux measured at the observed position is given for the cases of confusion, as well as an eventual short note.

3. Discussion on individual galaxies.

NGC 20 : This is the only galaxy of our list having no measured redshift. No signal has been detected in the velocity interval (4000, 6000 km s^{-1}) to the limit of 1 Jy km s^{-1}.

NGC 128 : No emission has been detected from this galaxy. But, in the observation at 3.3′E from its centre along the main axis, we have obtained a strong absorption feature (Fig. 3). This negative signal can be confidently attributed to the presence of the Sdm-m galaxy UGC 348 in the corresponding comparison field. The accurately measured coordinates of this object are : $\alpha = 0^h32^m53^s.3$ and $\delta = +02°39'28''$ (1950) ; so this galaxy is at 2.5′ from the centre of our comparison field located at $\alpha = 0^h33^m02^s.7$, $\delta = +02°38'36''$ (1950), and an attenuation of its signal by a factor 5.4 is then expected in our observation if it is a point source for the Arecibo beam. This assumption seems correct since its UGC dimensions are 1.2′ × 1.2′. The HI flux measured in our profile is 1.9 Jy km s^{-1}, leading to a probable total flux of $F_H = 10.4$ Jy km s^{-1} after the correction for beam attenuation ; this gives a HI mean density : $\sigma_H = 4.6 \times 10^{-3}$ g cm^{-2}, just the average value for its morphological type. On the other hand, $V_r = 4214$ km s^{-1} and $W_{20} = 160$ km s^{-1}. Its systemic velocity is therefore in agreement with a membership to the group of NGC 128, which contains NGC 126, 127 and 130 among others.

NGC 160 : This galaxy has already been detected in the HI-line at Nançay by Balkowski and Chamaraux (1983) ; but it was not possible to determine definitely whether the measurements were confused by the spiral UGC 354, that had an unknown redshift. As a matter of fact, the two objects are well separated by the Arecibo beam, since they are 5′ apart ; the HI parameters obtained at Arecibo and at Nançay are in excellent agreement, except perhaps for the HI fluxes, twice larger at Nançay than at Arecibo. This difference is probably due to the confusion with UGC 354 and to the finite HI extension of NGC 160. The Arecibo mapping of NGC 160 does not reveal any anomalous HI extension caused by an eventual interaction with UGC 354 ; but given the rather large velocity difference $\Delta V \sim 350$ km s^{-1} between the two objects, a strong interaction is not expected.

NGC 315 : This S0 galaxy is associated with a very extended radiosource, having a size of the order of one Mpc. At 21-cm, it is characterized by its surprisingly narrow absorption line centred at a velocity $V = V_{syst} + 490$ km s^{-1}, where V_{syst} is the systemic velocity of the galaxy ; this line has been observed in particular by Heckman *et al.* (1983). A study at high frequency resolution by Dressel *et al.* (1983) shows in fact that this line presents two components, 3 km s^{-1} apart, each of them having a 2.5 km s^{-1} half-width ; Dressel *et al.*

(1983) interpret these two narrow absorption features as due to two individual HI clouds covering completely the very small central radiosource (0.5 pc) of the galaxy, and in process of falling towards the centre of the galaxy.

Our observations show this narrow absorption at 5419 km s^{-1} (Fig. 4), in agreement with Dressel *et al.* (1983) within our 8.4 km s^{-1} resolution ; the area under the line is 0.92 Jy km s^{-1}, in excellent agreement with Dressler *et al.*'s value.

In addition, our observations reveal a second possible absorption feature, at $V = 4958 \text{ km s}^{-1} \pm 20 \text{ km s}^{-1}$ (i.e. $V_{syst} + 36 \text{ km s}^{-1}$), with a width at 20 % of the maximum : $W_{20} = 206 \pm 40 \text{ km s}^{-1}$ and an area $A = 0.54 \pm 0.2 \text{ Jy km s}^{-1}$. These parameters are in good agreement with those of the probable absorption feature detected by Heckman *et al.* (1983), and its existence can then be considered as quite likely. The corresponding column density is : $N_H = 0.9 \times 10^{20} \text{ cm}^{-2}$ taking $S = 1.1$ Jy for the flux density of the continuum source at 1400 MHz (Heckman *et al.*, 1983) and a spin temperature $T_s = 100$ K for HI. No HI emission has been detected from the galaxy.

NGC 1167 : This S0 galaxy has large apparent dimensions (3.3′ × 2.3′), so we have measured it at one beam each side from its centre along its major axis, and along its minor axis as well.

The profile observed at the central position has the classical double horn shape ; the parameters we derive from it are in good agreement with those found by Heckman *et al.* (1983), but we have obtained a better signal-to-noise ratio.

The profiles off centre show two peculiarities (Fig. 2 and Tab. I) :

(1) The fluxes obtained along the minor axis are significantly larger than those found along the major axis by 40 % ± 15 % (accounting for observational uncertainties). Thus the HI distribution is unusual, in the sense that there is more HI along the minor axis than along the major one, or, alternately, that the HI distribution has been stretched along the N-S direction. An obvious cause for such a phenomenon could be tidal effects due to companions. As a matter of fact, there are two disk galaxies companions of unknown redshifts at 2.0′ and 2.6′ from the point e3.3 and one compact object at 0.9′ from N3.3. Note that the expected HI fluxes of the companions do not seem to be sufficient to explain the excesses of flux observed, and, anyway, the shapes of the profiles e3.3 and N3.3 show no evidence of any contamination ; but tidal effects are by no means excluded.

(2) The two profiles at ± 3.3′ from the centre along the main axis are reduced to narrow peaks having their maxima at the two extremal velocities observed in the central profile. This means that in E3.3 and W3.3, one can only see the HI moving at the extremal rotation velocities in the galaxy. This situation can be explained in two ways :

(i) The HI is concentrated in a rotating ring, as found in several S0's by van Woerden *et al.* (1983). From (1), this ring is elongated along the minor axis or it is not in the plane of the galaxy. In both cases, this structure is unstable and should be rapidly destroyed, except if the ring is in a polar orbit.

(ii) The rotation curve of the galaxy is flat from a distance r_0 from its centre to at least 4′ ; the points located at distances lower than r_0 from the centre are not seen from W3.3 and E3.3, as expected since they must be well inside the 1.6′ optical radius of the object. Then from W3.3 and E3.3, one sees mainly regions of the galaxy rotating at the maximum rotational velocity V_{max}, not far away from its main axis, hence the peaks observed at $V = V_{syst} \pm V_{max} \sin i$ (i being the inclination of the galaxy).

Although it is impossible to choose between the two interpretations without a detailed mapping, one can note however that the ring hypothesis requires very special and transient conditions, contrary to the flat rotation curve explanation.

NGC 2911 : This galaxy possesses a compact radiosource in its nucleus, the flux being 130 mJy and the diameter 8 milliarcsec (Condon and Dressel, 1978 ; Crane, 1979). For this reason NGC 2911 has been observed by Mirabel (1983) in the 21-cm line, in order to detect an eventual HI absorption. The profile he has obtained at Arecibo is in total agreement with the one we find in the observation at the centre of the galaxy. The noticeable features in those profiles are the presence of a hole at $V \sim 3300 \text{ km s}^{-1}$ and a secondary bump at $\sim 3400 \text{ km s}^{-1}$. Mirabel examines two possible interpretations of these features : (a) An HI absorption at $\sim 3300 \text{ km s}^{-1}$; (b) a blended emission from two galaxies in the telescope beam. Since he has not noticed any other galaxy in the beam on the Palomar Sky Survey prints, he favours the first expalanation. However our mapping of NGC 2911 allows us to choose definitely between the two interpretations.

(a) The HI absorption :

Since the radiosource is exactly at the centre of the galaxy and since it is a point-source for the Arecibo radiotelescope, one expects the depth of an eventual absorption to be attenuated by the response of the beam in the West 2′ and East 2′ positions, i.e. by a factor of 3. But instead we observed no attenuation at all in the East 2′ position and, on the contrary, no absorption at all in the West 2′ position.

Therefore the hypothesis of the HI absorption is definitely ruled out.

(b) The blended emission :

The RC2 notes the presence of NGC 2912 at 1.3′ from the centre of NGC 2911, therefore in the Arecibo beam

(Fig. 5) ; no redshift is available for this object. On the PSS prints, NGC 2912 appears as a small very blue object (blue diameter $\sim 0.3'$) of low surface brightness, without any peculiar structure, therefore resembling a dwarf irregular. Thus a weak and narrow HI line is expected from such an object, corresponding very well to the narrow bump at ~ 3400 km s^{-1} observed at the central position N2911 0. In the position N2911 E2, NGC 2912 is at 1.8′ from the centre of the beam ; then a signal is still expected at the same velocity, as really found.

Now if we interpret the profiles N2911 0 and N2911 E2 as the sum of the contributions of the galaxies NGC 2911 and NGC 2912, it is possible to separate the two signals. Indeed noting that the left part of the HI line observed at the centre of NGC 2911 has the classical double horn structure, one can extrapolate the steep slope of the high velocity horn and derive the profile of NGC 2912 by subtraction. This procedure gives the HI parameters of NGC 2912, and of NGC 2911 as well. These quantities are reported in table I. After the offset beam correction of 1.3′, one obtains finally 0.7 Jy km s^{-1} for the HI flux of NGC 2912. Then note that the HI mean surface density of this galaxy is : $\sigma_H \sim 4.2 \times 10^{-3}$ g cm^{-2}, in excellent agreement with $\bar{\sigma}_H = 5 \times 10^{-3}$ g cm^{-2} found for late-type galaxies (Bottinelli *et al.*, 1982), making plausible the hypothesis of the blended emission ; at its redshift distance, the diameter of the dwarf would be of ~ 3 kpc (with $H_0 = 100$ km s^{-1} Mpc^{-1}), comparable to that of the Small Magellanic Cloud, also in agreement with the low internal velocity dispersion.

Thus the interpretation of our observations by the presence of the dwarf companion NGC 2912, possibly a satellite of NGC 2911, is in agreement with all the observed features, in particular also with the absence of any peculiarity in N2911 W2, since NGC 2912 is then out of the beam.

Adopting this interpretation, note that our profiles N2911 0, N2911 E2 and N2911 W2 also show that the centroid of the HI distribution is at the West of the optical centre. This is indicated by the asymmetry of the two horns and the absence of HI at low velocities ($V < 2900$ km s^{-1}) in the central profile, and by the HI flux higher in W2 than in E2. An obvious reason of such an asymmetry can be the presence of NGC 2914, at ~ 40 kpc from NGC 2911 and nearly at the same velocity. Because of this asymmetry, the presence of a signal in the E4 position, and the absence of it in the W4 position is rather surprising. But the spiral NGC 2914 is at 1.4′ from the E4 position, and it is likely that the HI signal at this point comes from this galaxy. In fact, if one attributes all the flux in E4 to NGC 2914 seen offset, one finds an HI surface density $\sigma_H \sim 1.3 \times 10^{-3}$ g cm^{-2} for this galaxy, in excellent agreement with its Sa type. For this reason, the profile E4 has not been considered in the computation of the HI diameter of NGC 2911 carried out in section 4.

NGC 2968 : Although classified with a zero type, this object is not an S0/a spiral according to RC2, but belongs to the rare class of the Irregular II (or I0) galaxies, which exhibit a large diversity of HI contents (Fouqué, 1982).

The profile obtained at the central position has a peculiar shape, very similar to the one observed in NGC 2911, i.e. a double horn feature associated with a little emission peak. In the present case too, the superimposition of the profiles of two galaxies is the only possibility worth examining to explain that peculiar shape ; indeed the absorption hypothesis is ruled out since NGC 2968 has not been detected as a radiosource at 21-cm (Hummel, 1980), and there is no galaxy in our comparison field. As a matter of fact, NGC 2968 is in pair with the spiral NGC 2964, which is located at 6.2′ SW (Fig. 6). The redshifts of the two galaxies have been measured optically by several authors, the values are in good agreement, giving $\bar{V}_r = 1598 \pm 50$ km s^{-1} for NGC 2968 and $\bar{V}_r = 1308 \pm 30$ km s^{-1} for NGC 2964. These are almost the recession velocities of the double horn feature ($V = 1352$ km s^{-1}) and of the little peak ($V = 1616$ km s^{-1}) of our profile N2968 0. Therefore the most straightforward interpretation of this profile is to assume that the double horn structure comes from HI associated with NGC 2964 and that the small peak is produced by NGC 2968. Since the angular distance between NGC 2964 and NGC 2968 exceeds much the dimensions of the Arecibo beam and those of the two galaxies, we cannot settle firmly on this interpretation without a detailed HI mapping of the region, which is not available up to now. Our assumption needs indeed a large anomalous extension of HI for NGC 2964 towards NGC 2968, otherwise no HI from NGC 2964 could be detected at Arecibo at the position of NGC 2968. However, as a matter of fact, evidence of such an extension is available from other HI observations.

Krumm and Salpeter have observed NGC 2964 at Arecibo at its centre and at $\pm 2'$ away along the main axis ; from these measurements, they have derived a total HI flux $F_H = 15$ Jy km s^{-1} and an HI extension along the main axis comparable to the optical one. However, HI measurements of this galaxy, with the NRAO 91-m radiotelescope by Peterson (1979), and Thuan and Martin (1981) have led to $F_H = 22$ Jy km s^{-1}, i.e. 50 % more, indicating an HI extension seen with the NRAO 10.8′ beam. Moreover, HI observations at the centre of NGC 2968 with the same radiotelescope (Huchtmeier, 1982) give a profile width and a central velocity similar to what is observed for NGC 2964, with in particular little HI if any at $V > 1530$ km s^{-1} ; that shows that NGC 2968 contributes very little to this profile, which is then mainly due to NGC 2964. The flux obtained in that position is : $F_H = 22$ Jy km s^{-1}, whereas

half this value would be expected because of beam attenuation if the HI of NGC 2964 were mainly concentrated within its optical limits. Finally Balkowski and Chamaraux (1983) have observed NGC 2964 with the Nançay radiotelescope (HPBW is 3.6′ in right ascension and 22′ in declination) ; they have obtained a flux of 16 Jy km s^{-1}, not much higher than the value 13.3 found at the central position by Krumm and Salpeter at Arecibo, showing that the extension of NGC 2964 is not within the Nançay beam, i.e. not North of the centre of the galaxy.

From all these observations, we conclude to the probable existence of a large HI extension to NGC 2964, extending mainly from the East of NGC 2964 towards NGC 2968, and emitting an HI flux of the order of 15 Jy km s^{-1}, i.e. as much as the main body of NGC 2964. This extension could be due to tidal effects between NGC 2964 and NGC 2968.

In these conditions, we expect indeed to detect a little part of this extension when observing NGC 2968 at Arecibo, as actually found. Note also that the positions of the horns of the profile N2968 0 and its width coincide very well with the corresponding features seen in the NRAO profiles, which is in favour of our interpretation.

The decomposition of the profile N2968 0 according to this interpretation leads to the HI parameters of NGC 2968 given in table I. The profile N2968 E3.3 still shows the extension of NGC 2964, strongly attenuated however ; no decomposition of this profile is possible ; note only that the high velocity part is reinforced compared to N2968 0, due either to the contribution of the S0 galaxy NGC 2970 ($V_r = 1678$ km s^{-1}), or to an excentred HI distribution in NGC 2968, because of tidal effects.

Note finally that a maximum rotational velocity $V_M = 87$ km s^{-1} can be derived for NGC 2968 from the width found for its HI profile and its 47° inclination. Adopting $H_0 = 100$ km s^{-1} Mpc^{-1}, the linear diameter of this galaxy is $A_0 = 9.9$ kpc and its blue absolute magnitude $M_B = -18.5$. With these values, NGC 2968 is located very close to the Tully-Fisher relations (A_0, V_M) and (M_B, V_M) given by Bottinelli *et al.* (1983). On the contrary, if the whole profile N2968 0 was produced by NGC 2968 alone, this galaxy would not follow the Tully-Fisher relation. This result gives some additional weight to our treatment of the profile N2968 0.

NGC 3226 : This elliptical galaxy is interacting with the Seyfert Sa galaxy NGC 3227, located at 2.3′ South ; then confusion is expected at Arecibo. The profile obtained in the position of the centre of NGC 3226 exhibits a double horn structure, typical of a rotating spiral, and also unusual wings in the high velocity part, beyond the steep descent of the high velocity horn. The central velocity of the double horn profile is 1129 km s^{-1}, very close to that of 1152 km s^{-1} measured optically for NGC 3227 ; in turn, the systemic velocity of NGC 3226 is 1356 km s^{-1}, i.e. at the high velocity end of the observed profile. So it is likely that the double horn profile comes essentially from the spiral galaxy NGC 3227, NGC 3226 giving perhaps the small contribution corresponding to the high velocity wings. Therefore no valuable information can be derived from our profile concerning the HI parameters of NGC 3226.

If this hypothesis is correct, then the very symmetrical double horn shape of the profile obtained at the position of NGC 3226 is unexpected, since this position is out of NGC 3227 along its main axis. This property seems then to imply that the HI distribution of NGC 3227 is displaced toward NGC 3226, probably because of the gravitational interaction between the two galaxies. As a matter of fact, the partial mapping of these two objects carried out at Arecibo by Knapp *et al.* (1978) shows clearly this displacement ; indeed the profile they obtain at the position of NGC 3227 is asymmetrical, with a peak at the position of the high velocity horn, characteristic of a rotating disk galaxy observed off centre along its main axis. The total flux measured by Huchtmeier and Bohnenstengel (1975) for the whole system is : $F_H = 28.3$ Jy km s^{-1}, i.e. 4 times ours. If the HI signal comes mainly from NGC 3227, then, the mean HI surface density of this galaxy would be : $\sigma_H \sim 0.7 \times 10^{-3}$ g cm^{-2}, in excellent agreement with its Sa type.

All these properties are in agreement with an origin of the neutral hydrogen from NGC 3227 mainly, its distribution being strongly disturbed by NGC 3226.

NGC 3986 : The Sc galaxy IC 2978 is at 4.6′ West from NGC 3986, nearly along its main axis, and very close to the position W4 (see Fig. 7). It has no known redshift, but if it is a physical companion of NGC 3986, then problems of confusion are expected to arise in the mapping of the West side of NGC 3986 and need a careful examination of the profiles.

No signal has been detected at 4′E from the centre of NGC 3986 along its main axis ; so no signal is expected to be observed from this galaxy in the symmetrical position W4, if at least the HI distribution in this object is reasonably symmetrical. Then one can make the provisional assumption that the signal observed in N3986 W4 comes mainly from IC 2978, which is only 0.8′ from this point. Is this hypothesis compatible with observations ?

The profile observed in the position N3986 W4 has the classical double horn shape, characteristic of a late-type galaxy ; the low velocity horn is higher than the high velocity one, which can be understood since the galaxy is seen edge-on, and the East extremity of its main axis is nearer to W4 than the West one. The observation in the position N3986 W3.3 (not shown in Fig. 2) confirms that view, since one finds there the low velocity horn only and one is actually on the East side of IC 2978. On the other hand the HI flux of the profile N3986 W4 is 2.6 Jy km s^{-1} ; if this signal comes mainly from IC 2978,

this value leads to an HI flux from this galaxy $F_H = 2.8$ Jy km s^{-1}, after correction for the 0.8′ offset ; then one expects fluxes of 1.6 Jy km s^{-1} in the W3.3 and W6 positions, which are 1.5′ distant from the centre of IC 2978 (this galaxy is not extended compared to the beam), in total agreement with fluxes of 1.6 and 1.8 Jy km s^{-1} respectively measured at these points.

Thus we can conclude that the signals measured in the positions W3.3, W4 and W6 are essentially due to the galaxy IC 2978, and not to NGC 3986. Moreover, with our F_H value, we obtain for IC 2978 : $\sigma_H = 2.0 \times 10^{-3}$ g cm^{-2}, close to the average value $\bar{\sigma}_H = 2.4 \times 10^{-3}$ g cm^{-2} for the Sc galaxies (Bottinelli *et al.*, 1982) ; at last the diameter of this object is of the order of 10 kpc, and its rotational velocity of 100 km s^{-1}, in very good agrement with the Tully-Fisher relation (Bottinelli *et al.*, 1983).

The presence of IC 2978 also allows to explain the strange appearance of the profile N3986 W2. Indeed, on the basis of profiles N3986 0 and N3986 E2, one expects for N3986 W2 a peak in the high velocity side (as actually observed at 3500 km s^{-1}) followed by a decrease of the signal towards the low velocity side, as usual for edge-on galaxies observed off centre along their main axis and as obtained symmetrically in E2. Then the peak at 3200 km s^{-1} is rather unexpected, but in fact it is exactly at the same velocity as the low velocity horn of IC 2978 ; W2 is at 2.0′ from the East side of the galaxy, so an attenuation of the height of the peak of about a factor three is expected in W2, compared to what is observed in W4 ; this corresponds well to the observations.

NGC 4169 : This S0 galaxy forms with the spiral galaxies NGC 4174 and NGC 4175 a compact triplet at $\bar{V} \sim 3900$ km s^{-1} (Fig. 8). The galaxy NGC 4173, although very close to the triplet in projection, is in fact a foreground object, at $V \sim 1100$ km s^{-1}.

The line profile obtained at the position of NGC 4169 is centred close to the optical velocity of the galaxy ; it exhibits the usual double horn structure, but it is definitely asymmetrical, the high velocity horn having a greater intensity than the low velocity one (Fig. 2). That is far too important to result from the ~ 20″ pointing uncertainty, but it could be caused by an HI distribution excentred compared to the light, or/and by confusion with NGC 4174 and NGC 4175, which are located at 2.5′ and 2.8′ from NGC 4169 respectively, and have indeed recession velocities in the zone of the high velocity horn of NGC 4169. The available evidence shows both processes can well operate, especially the second one. Indeed first the profile obtained at the position of NGC 4175 has a central velocity, a width and horn positions very close to what is observed in the high velocity horn of N4169 (Fig. 2) ; the extra-intensity in this feature can then be accounted for, at least partially, if not totally, by the gas of NGC 4175 seen from the position of NGC 4169. On the other hand, Sulentic and Arp (1983) have carried out at Arecibo HI observations near NGC 4173, at 2.4′ North from NGC 4169. The profiles they have obtained have the same central velocities and the same widths as the one we have found at the centre of NGC 4169 ; therefore they are likely to be produced mainly by the neutral hydrogen of that galaxy. But, unexpectedly, their corresponding HI fluxes are as high as 80 % of that obtained in our N4169 profile. This means that the HI distribution in NGC 4169 is not centred at the optical centre, due to tidal effects for instance, hence another possible cause for the asymmetry observed in the profile of NGC 4169. Whatever it may be, this last circumstance prevents us to compute the total HI mass of NGC 4169 in the lack of a very detailed mapping of the whole triplet ; only a lower limit can be tentatively estimated, which leads to $\sigma_H > 10^{-3}$ g cm^{-2}, a high value for an S0 galaxy (Chamaraux *et al.*, 1986), which could be explained by gas accretion from other triplet members.

NGC 4309 : Possible detection at $V \sim 1050$ km s^{-1}, with a flux $F_H \sim 0.3$ Jy km s^{-1}. If the detection is real, this galaxy would be the S0 with the lowest HI mean surface density ever measured ($\sigma_H \sim 0.05 \times 10^{-3}$ g cm^{-2}).

NGC 6014 : Possible detection at $V \sim 2400$ km s^{-1}, $F_H \sim 0.3$ Jy km s^{-1}, leading to $\sigma_H \sim 0.06 \times 10^{-3}$ g cm^{-2}, a value nearly as low as for NGC 4309.

UGC 10528 : This galaxy has been observed at Arecibo at its central position by Haynes and Giovanelli (1984), leading to HI parameters very close to those we obtain for the profile U10528 0.

One can note the peculiar shape of the profiles obtained at 3.3′ East and West of the galaxy centre. In W3.3, only a narrow emission is observed, at the exact position of the low velocity horn of the central profile. In E3.3, a peculiar two peaks structure is observed ; such a structure could be artificially created by HI in the comparison field, which seems however to be ruled out since no galaxy is visible there. Thus we think that the two peaks are real ; the lower velocity one is at the position of the high velocity horn of the central profile. So the other peak is out of the velocity range covered by the central profile ; it does not contain however HI at velocities higher than the escape velocity $V_e = 4680$ km s^{-1} from the galaxy, and is then likely to be produced by matter gravitationally bound to U10528. No galaxy is visible in the Arecibo beam ; thus this peak could result from a high velocity HI cloud in the galaxy. Its HI mass is at least $\sim 4 \times 10^8 M_\odot$ (taking $H_0 = 100$ km s^{-1} Mpc^{-1}) ; assuming it is in dynamical equilibrium, the virial theorem gives a diameter of about 600 pc for this cloud, i.e. 20 % of the galaxy size.

In fact, if we put aside the high velocity HI cloud, which does not participate in the rotation of the disk, we can see that we are in the same situation encountered for NGC 1167, i.e. only a narrow emission peak at the

extremal rotation velocity in E3.3 and W3.3. As discussed above, such a peculiarity can have two possible causes : either a flat rotation curve to at least $\sim 4'$ from the centre, or the HI mainly concentrated in a ring. The diameter of this eventual ring can be determined by noting that the narrow peaks observed in E3.3 and W3.3 and the horns obtained in the central profile are emitted by the same regions of the ring, namely those located on the main axis of the galaxy. The difference between their respective intensities is then due to different attenuations by the beam when pointing at the centre of the galaxy, and at E3.3 and W3.3, respectively ; hence the position of those regions on the main axis. Assuming the ring circular and in the plane of the galaxy, we find then 2.4′ for its diameter, just the UGC diameter of the galaxy, in agreement with the dimensions of the HI rings found by van Woerden *et al.* (1983) around several S0 and S0-a galaxies.

To end this discussion, note that UGC 10528 has been measured by Hewitt *et al.* (1983) with the 91 m Green Bank radiotelescope, HPBW of which is 10.8′ at 21 cm ; they have obtained a total HI flux of 7.4 Jy km s^{-1}. This value is in good agreement with the total flux $F_H > 6.6$ Jy km s^{-1} found from our mapping (see next Sect.) and taking into account the feature in E3.3 ; since the exact position of this feature is unknown in the beam centered at E3.3, we can only derive a lower limit for its flux assuming it is exactly at E3.3.

NGC 6240 : This galaxy is associated with the radiosource 4C 02.44. It presents a peculiar morphology, and could in fact be formed by two interacting galaxies.

HI 21-cm observations at Arecibo by Heckman *et al.* (1983) have revealed the existence of a very wide deep absorption line in this object. These authors give for the line a 20 % width $W_{20} = 700 \pm 160$ km s^{-1}, whereas Baan *et al.* (1985)'s profile (also obtained at Arecibo) leads to $W_{20} = 570$ km s^{-1}. In fact, on our original profile (Fig. 9(a)), it can be seen how difficult it is to determine accurately the extremities of the line. Subtraction of a third order polynomial leads to the line shown in figure 9(b). We find for it a 20 % width : $W_{20} = 490 \pm 100$ km s^{-1}, i.e. somewhat lower than the other determinations, a mean redshift $V = 7298$ km s^{-1} (i.e. exactly V_{syst}) and an area $A = 6.8$ Jy km s^{-1}, which leads to a column density :

$$N_H/T_s = 5.4 \times 10^{19} \text{ cm}^{-2} \text{ K}^{-1}$$

(continuum flux of 230 mJy), in agreement with the value 4.7×10^{19} cm^{-2} K^{-1} given by Baan *et al.* (1985).

N 7280 : This galaxy is in pair with a dwarf irregular companion at 4.7′NE (Fig. 10). It has already been detected at Arecibo by Biermann *et al.* (1979) ; we confirm its HI parameters with a signal-to-noise ratio better than theirs.

Our observation at 3.3′W gives no detectable signal, but the one at 3.3′E leads to a definite narrow profile ; if the HI distribution in NGC 7280 is reasonably symmetrical, it is natural to attribute this profile to the dwarf companion, which is 1.7′ from the point E3.3. A confirmation of this conclusion is given by a Westerbork mapping of NGC 7280, which has shown a centrally concentrated HI distribution in this galaxy (Van Driel, private communication). We derive a corrected flux for the companion : $F_H = 3.2$ Jy km s^{-1}, after correction for the beam offset. Note that Fisher and Tully (1981) have observed the dwarf companion with the Green Bank 91 m radiotelescope ; they have measured a flux of 3.9 Jy km s^{-1}. If we substract the contribution of NGC 7280 seen at 4.7′ with their beam of 10.8′ HPBW, we find 3.3 Jy km s^{-1} for the HI flux of the dwarf companion, i.e. the value obtained from our offset observation, interpretation of which is so confirmed. This leads to $\sigma_H = 2.7 \times 10^{-3}$ g cm^{-2}, a normal value for a late type galaxy.

NGC 7803 : This object, classified S0-a in UGC, is the brightest one in a chain of six galaxies (Fig. 11) ; the axis of the chain is roughly East-West, as the main axis of NGC 7803. Except this galaxy, no member of the chain has a known recession velocity.

As seen in figure 11, each galaxy of the chain — except perhaps E — can contribute to at least two of the line profiles observed in the positions N7803 0, E3.3 and W3.3, and confusion can occur. It is not possible to derive the HI flux of NGC 7803 from the fluxes obtained in each of these profiles, even if we take advantage of the fact that all the objects should be point sources for the Arecibo instrument (diameter $\leqslant 1'$) ; indeed such a derivation would need to solve a system at five unknown, and only three equations are available. All that can be said is that the HI flux of NGC 7803 is likely to be lower than the value 2.85 obtained for N7803 0, resulting in $\sigma_H < 1.7 \times 10^{-3}$ g cm^{-2}, which is quite normal for a S0-a type (Chamaraux *et al.*, 1986).

On the other hand, note the weak profile observed in W7.3, whereas no galaxy of the chain is at less than 6.2′ from this point, and cannot give any emission there if it is a point source. Therefore, if this emission is real, it means that there is extended HI within the chain, to about 100 kpc from NGC 7803, the existence of this diffuse gas resulting probably from tidal effects.

At last note that the total flux observed in the different points is about 6.5 Jy km s^{-1}. This value is in good agreement with the one of 8.0 Jy km s^{-1} obtained by Davis and Seaquist (1983) from Green Bank 91 m radiotelescope measurements ; in fact, given the HPBW of this instrument, the value found by Davis and Seaquist is practically the sum of the fluxes of the 6 galaxies of the chain, and is expected to be slightly higher than ours. Note that Peterson (1979) has measured $F_H = 4.1$ Jy km s^{-1} with the 91 m radiotelescope, too, but his

signal-to-noise ratio is poor, and he has apparently missed the low velocity part of the profile, perhaps because of curvature.

4. Derivation of the HI diameters and of the total fluxes for six mapped galaxies.

Nine of our program galaxies have been detected in other positions than in their centre, generally at several points along the optical main axis. For three of them (NGC 2968, NGC 7280 and NGC 7803), those observations cannot be used to determine an HI diameter, because of confusion. But this parameter, as well as the total flux, can be derived for the other six objects.

The principle of the method we have adopted for this calculation is the same as the one used by Hewitt *et al.* (1983). Namely we describe the large-scale distribution of the neutral hydrogen in the plane of the galaxy by a function having a given realistic shape, and which depends on the gas extension and on the HI central density σ_0 as free parameters. One can then compute the HI fluxes $F_H(x)$ at the different points observed along the main axis and located at a distance x from the centre of the galaxy ; in the models used, the ratios $\rho(x) = F_H(x)/F_H(0)$ depend only on the HI diameter D_H of the distribution, hence this quantity from comparison between observed and computed values of $\rho(x)$. From D_H we then compute the ratio $F_t/F_H(0)$ of the total HI flux emitted by the galaxy to the flux observed at its centre, hence F_t.

The HI distribution in the plane of the galaxy is defined by the function $\sigma_H(r)$ of the distance r to the centre of the object, where σ_H is the HI surface density. After a few trials, we have adopted for $\sigma_H(r)$ a Gaussian function :

$$\sigma_H(r) = \sigma_0 \exp(-r^2/\theta_1^2) . \quad (2)$$

Although this model does not match the central HI hole observed in the spirals (especially in the early ones), it leads here to the same results as the double Gaussian with a central hole used by Hewitt *et al.* (1983). The reason is that our galaxies have not a large HI extension, and the hole size is accordingly small and is smeared out by the Arecibo beam.

In this model, the HI diameters D_{50} and D_{70} of the HI disks containing 50 % and 70 % of the total HI mass respectively, are given by : $D_{50} = 1.67\ \theta_1$ and $D_{70} = 2.20\ \theta_1$.

On the other hand, one has for the expression of the HI flux $F_H(x_0)$ measured at a point of the major axis of the galaxy located at the abscissa x_0 from its centre :

$$F_H(x_0) = \frac{\alpha}{D^2} \iint \sigma_H(x, y)\, B(x - x_0, y)\, dx\, dy , \quad (3)$$

where α is a constant depending on the units, D the distance of the galaxy, x and y the current coordinates along the two axes of the galaxy, and $B(\xi, \eta)$ the response of the normalized beam supposed centred at $(0, 0)$.

Hence :

$$\frac{F_H(x_0)}{F_H(0)} = \frac{\iint \sigma_H(x, y)\, B(x - x_0, y)\, dx\, dy}{\iint \sigma_H(x, y)\, B(x, y)\, dx\, dy} . \quad (4)$$

$\sigma_H(x, y)$ is easily computed from $\sigma_H(r)$ accounting for the inclination i of the galaxy on the line-of-sight ; since the point (x, y) comes from the point $(x, y/\cos i)$ in the plane of the disk, one obtains immediately :

$$\sigma_H(x, y) = \frac{\sigma_0}{\cos i} \exp[-(x^2 + y^2/\cos^2 i)/\theta_1^2] .$$

Since our mappings never extend very far away from the centres of the galaxies, the Gaussian expression is excellent to describe the beam pattern, and we have consequently used for $B(x, y)$ the expression :

$$B(x, y) = \exp[-(x^2 + y^2)/\theta_B^2] , \quad (5)$$

where θ_B is the half-width of the beam at $1/e$ of its central value. θ_B is 1.9′ for the circular feed and 2.3′ for the flat feed (corresponding to HPBW of 3.2′ and 3.9′ respectively).

Then the integrals (3) and (4) can be computed analytically ; we obtain :

$$\rho(x_0) = \frac{F_H(x_0)}{F_H(0)} = \exp[-x_0^2/(\theta_1^2 + \theta_B^2)] . \quad (6)$$

And :

$$\frac{F_t}{F_H(0)} = [1 + (\theta_1/\theta_B)^2]^{1/2}\, [1 + (\theta_1 \cos i/\theta_B)^2]^{1/2} \quad (7)$$

hence D_{50}, D_{70} and F_t.

(6) gives θ_1 for each point x_0 observed. For a few galaxies (especially NGC 3413 and NGC 5587), a slight HI asymmetry appears between the two mapped sides of the object. Such an asymmetry is not necessarily intrinsic, but can be produced by the 20″ pointing uncertainty, since a mere 30″ error on the position of the point observed off centre can lead to the effects found. For NGC 3413 however, the HI asymmetry is likely to be real, since it is observed in the same direction at 2′ and at 4′ from the centre. If the cause of the asymmetry is a pointing error or a slight displacement of the centre of the HI distribution with respect to the optical one, it can be easily shown that θ_1 and F_t remain nearly unchanged if we symmetrize the distribution, i.e. if we replace $F_H(x_0)$ and $F_H(-x_0)$ by

their geometrical average. Thus we have adopted this procedure for all the cases of possible asymmetries. For NGC 2911, we have used the previous discussion to remove from the flux in W2 the contribution of NGC 2912. For NGC 3986, the flux in W2 comes partly from IC 2978, as explained in the previous section ; therefore we have taken $F_H(W2) = F_H(E2)$ for this galaxy ; at last, for NGC 5587, we have not considered the measurements at 4.8′ from the centre, since we have a detection at E4.8 only.

For NGC 3413, we obtain two values for θ_1 since we have measurements at two couples of points $(-x_0, x_0)$. The final value of θ_1 adopted is the average of those two values, weighted by $1/\sigma^2$, where σ is the uncertainty on the value θ_1 due to the uncertainties on the fluxes.

The inclinations i have been computed as explained by Bottinelli *et al.* (1983) ; for NGC 3986, an inclination of 90° has been adopted. There are some problems with NGC 1167, since its HI flux is stronger at 3.3′ along the minor axis than at 3.3′ along the major axis. One possible reason for this is that the HI plane makes some angle with the stars plane. Therefore the HI diameter and the total flux we obtain for this galaxy have to be taken with caution ; these parameters have been computed using the major axis data exclusively.

The HI diameters, the total HI fluxes as well as the parameters needed for their computations are given in table II.

Note that we have checked that our models give actually no detectable HI at the points where no detection has been obtained. At last the uncertainty on the diameters due to the uncertainty on the fluxes alone is about 0.2′.

A quantity of interest is the ratio D_{50}/a_0 of the HI D_{50} diameter of the galaxy to its optical one. Indeed Fouqué (1983) has shown that this ratio varies continuously along the morphological sequence ; for 8 S0 galaxies, he obtains : $\overline{\log D_{50}/a_0} = 0.15 \pm 0.09$. Adding our four new HI diameters of S0 galaxies (NGC 1167 has been excluded after the previous discussion), we find :

$$\overline{\log D_{50}/a_0} = 0.08 \pm 0.07 \quad \text{for} \quad 12 \text{ S0's} .$$

This leads to : $\overline{D_{70}/a_0} \sim 1.6$ a value a little larger than the average value of 1.2 obtained by Hewitt *et al.* (1983) for the spiral galaxies.

5. Conclusions.

In order to obtain a complete sample of lenticular galaxies observed in the HI line at high sensitivity, we have carried out 21-cm line observations at Arecibo of 56 galaxies, mostly S0's. Twelve S0's and four S0-a have been detected, among which 12 for the first time. In addition, 9 of these objects have been successfully mapped along their main axis.

A thorough discussion of the observations of several individual objects has allowed to solve some cases of confusion, in particular for the mapped S0's NGC 2911, NGC 2968, and NGC 3986. For NGC 2911, the HI absorption proposed by other authors is definitely ruled out ; we have also found evidence for two possible cases of HI ring structures or flat rotation curves in the S0's NGC 1167 and UGC 10528. This discussion shows the exceptional capabilities of the Arecibo radiotelescope in order to disentangle the confusion problems, mainly thanks to its high sensitivity.

For six of the mapped galaxies, a very simple deconvolution procedure has been used in order to derive their HI diameters and their total HI fluxes. For a given optical diameter, the HI diameter of an S0 appears to be 30 % ± 20 % larger on an average than for a spiral.

Acknowledgements.

We thank the referee of this paper, H. van Woerden, for a very careful critical reading of the manuscript, having resulted in several helpful comments and suggestions.

One of us (C. B.) warmly thanks W. Sargent and the California Institution of Technology for support and hospitality during the year the first observing run was performed. C. B. thanks also the Physics Department at the University of California, Irvine for hospitality at the time of the second observing run.

References

Baan, W. A., Haschick, A. D., Buckley, D., Schmelz, J. : 1985, *Astrophys. J.* **293,** 394.
Balkowski, C., Chamaraux, P. : 1983, *Astron. Astrophys. Suppl. Ser.* **51,** 331.
Bicay, M. D., Giovanelli, R. : 1986, *Astron. J.* **91,** 705.
Biermann, P., Clarke, J. N., Fricke, K. J. : 1979, *Astron. Astrophys.* **75,** 7.
Bottinelli, L., Gouguenheim, L., Paturel, G. : 1982, *Astron. Astrophys.* **113,** 61.
Bottinelli, L., Gouguenheim, L., Paturel, G., de Vaucouleurs, G. : 1983, *Astron. Astrophys.* **118,** 4.
Bridle, A. H., Davis, M. M., Fomalont, E. B., Lequeux, J. : 1972, *Astron. J.* **77,** 405.
Chamaraux, P., Balkowski, C., Fontanelli, P. : 1986, *Astron. Astrophys.* **165,** 15.
Condon, J. J., Dressel, L. L. : 1978, *Astrophys. J.* **221,** 456.
Crane, P. C. : 1979, *Astron. J.* **84,** 281.

DAVIS, L. E., SEAQUIST, E. R. : 1983, *Astrophys. J. Suppl. Ser.* **53,** 269.
DE VAUCOULEURS, G., DE VAUCOULEURS, A., CORWIN, H. C. : 1976, *Second Reference Catalogue of Bright Galaxies*, University of Texas (Austin).
DRESSEL, L. L., BANIA, T. M., DAVIS, M. M. : 1983, *Astrophys. J. Lett.* **226,** L97.
DRESSEL, L. L., CONDON, J. J. : 1976, *Astrophys. J. Suppl. Ser.* **31,** 187.
FISHER, J. R., TULLY, R. B. : 1981, *Astrophys. J. Suppl. Ser.* **47,** 139.
FOUQUÉ, P., 1982 : Thèse de Doctorat de troisième cycle — Université de Paris VII.
FOUQUÉ, P., 1983 : *Astron. Astrophys.* **122,** 273.
GALLOUËT, L., HEIDMANN, N. : 1971, *Astron. Astrophys. Suppl. Ser.* **3,** 325.
GALLOUËT, L., HEIDMANN, N., DAMPIERRE, F. : 1973, *Astron. Astrophys. Suppl. Ser.* **12,** 89.
GIOVANARDI, C., KRUMM, N., SALPETER, E. E. : 1983, *Astron. J.* **88,** 1719.
HAYNES, M. P., GIOVANELLI, R. : 1984, *Astron. J.* **89,** 758.
HECKMAN, T. M., BALICK, B., VAN BREUGEL, W. J. M., MILEY, G. K. : 1983, *Astron. J.* **88,** 583.
HEWITT, J. N., HAYNES, M. P., GIOVANELLI, R. : 1983, *Astron. J.* **88,** 272.
HUCHRA, J., DAVIS, M., LATHAN, D., TONRY, J. : 1983, *Astrophys. J. Suppl. Ser.* **52,** 89.
HUCHTMEIER, W. K. : 1982, *Astron. Astrophys.* **110,** 121.
HUCHTMEIER, W. K., BOHNENSTENGEL, H. D. : 1975, *Astron. Astrophys.* **44,** 479.
HUMMEL, E. : 1980, *Astron. Astrophys. Suppl. Ser.* **41,** 151.
KNAPP, G. R., KERR, F. J., WILLIAMS, B. A. : 1978, *Astrophys. J.* **222,** 800.
KRUMM, N., SALPETER, E. E. : 1980, *Astron. J.* **85,** 1312.
MIRABEL, I. F. : 1983, *Astrophys. J. Lett.* **270,** L35.
NILSON, P. : 1973, Uppsala General Catalog of Galaxies, *Uppsala Astron. Obs. Ann.* **1,** 6.
PALUMBO, G. G. C., TANZELLA-NITTI, G., VETTOLANI, G. : 1983, *Catalog of Radial Velocities of Galaxies*, Gordon and Breach Science Publishers (New York, London, Paris).
PETERSON, S. : 1979, *Astrophys. J. Suppl. Ser.* **40,** 527.
SULENTIC, J. W., ARP, H. : 1983, *Astron. J.* **88,** 489.
THUAN, T. X., MARTIN, G. E. : 1981, *Astrophys. J.* **247,** 823.
VAN WOERDEN, H., VAN DRIEL, W., SCHWARZ, V. J. : 1983, in « Internal Kinematics and Dynamics of Galaxies », *I.A.U. Symp.* No. **100,** E. Athanassoula (Ed.) p. 99.

TABLE I. — *21-cm line parameters for the observed galaxies.*

Name	P.A	r	T	a_o	V_{opt}	V_{HI}	$W_{20\%}$	$W_{50\%}$	F_H	Notes
	(°)	(')		(')	km s^{-1}	km s^{-1}	km s^{-1}	km s^{-1}	Jy km s^{-1}	
(1)	(2)	(3)	(4)	(5)	(6)	(7)	(8)	(9)	(10)	(11)
N 16	16	E 3.3	-3	2.0	3041				<0.64	
		W 3.3							<0.72	
N 20		0	-3	2.2					<0.99	*
N 80	-	0	-3	2.7	5698				<0.80	
		E 3.3							<1.67	
		W 3.3							<0.88	
N 125		0	0	2.0	5289	5306±44	367±72	264±58	0.99±.16	
N 128	1	0	-2	2.8	4243				<1.36	*
		E 3.3							<1.45	
U 348[c]		2.5	Sdm-m	1.3		4214	160	101	1.9	*
N 160	45	0	-1	3.0	5327	5255±3	545±5	520±5	3.56±.27	*
		E 3.3							<1.14	
		W 3.3							<1.11	
		e 3.3							<0.77	
U 354		0	Sb-c	0.9		5618±12	248±21	222±17	1.05±.09	*
N 315		0	-3	3.2	4921				<1.33	*HI absorption
I 89	-	0	-2	2.3	5437	5446±10	316±18	282±14	1.07±.10	
		E 3.3							<1.92	
N 467		0	-2	2.6	5467				<1.56	
N 499		0	-3	2.1	4375				<1.16	
N 661		0	-2*	2.3	3836				<0.57	
N 890		0	-3	2.9	4043				<0.89	
N 1167	70	0	-3	3.5	4723	4956±3	468±5	451±4	4.36±.34	*
		E 3.3				4781±3	119±5	68±4	1.75±.10	
		W 3.3				5139±4	119±6	60±5	1.83±.12	
		N 3.3				4960±25	442±42	400±34	3.12±.46	
		e 3.3				4896±19	281±31	213±25	2.26±.29	
		E 6.6							<2.00	
N 2563		0	-2*	2.4	4642				<0.55	
N 2911	140	0	-2	4.3	3254	3134(±1)	405(±2)	311(±2)	2.63(±.11)	*F_{tot} = 3.09
		E 2				3209(±3)	274(±5)	151(±4)	1.25(±.08)	F_{tot} = 1.92
		W 2				3043±6	538±10	244±8	1.97±.19	
		E 4				3199±35	563±57	521±46	1.14±.20	
		W 4							<0.80	
N 2912[c]		1.3	dwIrr?	0.4		3440(±6)	180(±11)	122(±9)	0.46(±.03)	*
N 2968	45	0	0	2.2	1600	1616(±17)	127(±28)	71(±23)	0.42(±.05)	*F_{tot} = 2.76
		E 3.3							(0.96)	F_{tot} = 1.83
N 3098		0	-2	2.1	1401				<1.58	
N 3226		0	-5*	2.9	1275	1169±3	514±5	398±4	6.79±.43	*confusion
N 3227		0	1	5.4	1200					
N 3245	177	0	-2	3.1	1370				<1.47	
		E 3.3							<0.68	
		W 3.3							<0.76	
N 3413	178	0	-2	3.8	628	645±1	190±1	157±1	10.28±.12	
		E 2				632±1	166±1	91±1	7.36±.09	
		W 2				657±1	166±1	108±1	5.24±.09	
		E 4				603±4	157±7	83±6	1.02±.07	
		W 4				638±27	191±44	168±36	0.67±.07	
I 2978[c]		0.8	Sc	1.0		3249(±9)	252(±16)	200(±13)	2.37(±.15)	*

TABLE I *(continued)*.

(1)	(2)	(3)	(4)	(5)	(6)	(7)	(8)	(9)	(10)	(11)
N 3986	110	0	-2	2.4	3242	3263±2	572±3	538±2	3.61±.19	*
		E 2				3221±7	454±11	143±9	1.60±.22	
		W 2				3276(±8)	547(±13)	471(±11)	2.17(±.28)	F_{tot} = 2.62
		E 4							<0.92	
		W 4				3213(±5)	320(±8)	202(±7)	2.56(±.20)	mainly due to IC 2978
		E 6							<0.91	
		W 6				3250(±47)	278(±75)	261(±61)	1.77(±.27)	partly due to IC 2978
N 4008		0	-2	2.4	3550				<0.63	
N 4073		0	-3	2.5	5966				<1.17	
N 4169		0	-2	2.0	3777	3811±2	473±4	405±3	4.54±.24	*possible
N 4175		0	Sb	1.6	4034	3933±4	313±8	237±6	3.30±.24	*confusion
N 4233		0	-1	2.1	2224				<0.52	
N 4292		0	-2	2.0	2258				<1.90	
N 4309		0	-1	1.9	1053				<0.66	*
N 4310	128	0	-1	2.3	901	913±5	199±9	174±7	1.15*±.08	
		E 3.3							<2.13*	
		W 3.3							<1.88*	
N 4339		0	-5	2.5	1287				<1.10	
N 4435	13	0	-2	2.9	773				<0.79	
		E 3.3							<0.60	
N 4620		0	-2	2.1	1214				<0.48	
N 4715		0	-1	2.0	6922				<1.06	
N 4849		0	-3	2.2	5885				<0.53	
N 4914		0	-3	3.5	4663				<1.26	
N 4931		0	-2	1.7	5849				<0.54	
N 5380		0	-3	2.3	3173				<1.26	
N 5444		0	-3	2.8	3974				<0.72	
N 5587	162	0	0	2.5	2294	2303±1	410±1	393±1	6.82*±.24	
		E 3.3				2210±3	226±6	67±5	1.96*±.22	
		W 3.3				2453±7	126±12	75±10	1.40*±.12	
		E 4.8				2244±36	187±58	112±47	0.56*±.19	
		W 4.8							<1.99*	
		E 6.6							<1.62*	
		W 6.6							<1.58*	
N 5838	43	E 3.3	-3	3.7	1359				<1.36	
		W 3.3							<1.10	
N 5846		0	-5	3.8	1709				<1.44	
N 5854	55	0	-1	2.2	1669				<1.56	
		W 3.3							<1.69	
N 5864		0	-2	2.4	1850				<0.54	
N 5865		0	S0	2.8	2042				<1.19	
N 5928		0	S0	2.6	4567				<1.34	
N 6014		0	S0	2.4	2429				<0.65	*
U 10528	65	0	S0	2.6		4267±3	508±4	491±4	4.98±.32	*
		E 3.3				(4553)	(195)	(161)	1.31	
		W 3.3				4059±6	93±11	51±9	0.51±.04	
N 6240		0	0	2.3	7298					*HI in absorption
N 6587		0	-3	2.9					<0.36	
N 6710		0	-1	2.2	4556	4552±4	560±7	501±6	0.81±.09	
N 7280	78	0	-2	2.5	1903	1846±4	250±6	184±5	1.06±.07	*
		E 3.3				1892±3	142±5	109±4	1.45±.04	entirely due to A2224+15
		W 3.3							<0.73	
A 2224+15		1.7	Dw Irr	0.9		1892(±3)	142(±5)	108(±4)	1.45(±.04)	*parameters of N 7280 E 3.3

TABLE I *(continued).*

(1)	(2)	(3)	(4)	(5)	(6)	(7)	(8)	(9)	(10)	(11)
N 7386	150	0	-2	2.2	7242				<0.45	
		E 3.3							<1.62	
N 7457	130	0	-3	4.3	525				<1.77	
		E 3.3							<1.24	
		W 3.3							<1.27	
		e 3.3							<0.87	
		w 3.3							<0.66	
N 7550		0	-2	1.8	5109				<0.54	
N 7623		0	-1	1.9	3674				<0.72	
N 7648		0	-2	1.8	3593	3559±83	329±130	202±104	0.42±.09	
N 7803	85	0	S0-a	1.1	5314	5336±2	325±4	233±3	2.85±.14	*confusion
		E 3.3				5307±13	264±23	239±18	0.79±.08	see discussion
		W 3.3				5367±2	213±3	120±3	2.23±.13	
		W 7.3				5422±21	256±36	162±29	0.55±0.8	

(See Sect. 2 for the explanations of the columns).

TABLE II. — HI *diameters and total fluxes for mapped galaxies.*

Galaxy	T	i	$F_H(0)$	x_o	$F_H(x_o)$	θ_B	θ_1	$\theta_1$def	D_{50}	D_{70}	D_{50}/a_o	F_t
		(°)	(Jy kms^{-1})	(')	(Jy kms^{-1})	(')	(')	(')	(')	(')		(Jy kms^{-1})
(1)	(2)	(3)	(4)	((5)	(6)	(7)	(8)	(9)	(10)	(11)	(12)	(13)
N 1167	-3	40	4.4	±3.3	1.8	1.9	2.9	2.9	4.9	6.4	1.4	12.1
N 2911	-2	43	2.6	±2.0	1.44	1.9	1.8	1.8	3.0	3.9	0.70	4.4
N 3413	-2	72	10.3	±2.0	6.2	1.9	2.1	1.9	3.2	4.2	1.5	15.3
"				±4.0	0.83	1.9	1.6					
N 3986	-2	90	3.6	±2.0	1.6	1.9	1.1	1.1	1.8	2.4	0.76	4.2
N 5587	0	75	6.8	±3.3	1.7	2.3	1.5	1.5	2.6	3.4	1.0	8.3
U 10528	-1	60	5.0	±3.3	0.5	1.9	1.0	1.0	1.7	2.3	0.67	5.8 *

Column 1 : Name of the galaxy : N for NGC, U for UGC.
Column 2 : De Vaucouleurs numerical morphological type.
Column 3 : Inclination.
Column 4 : HI flux measured at the central position.
Column 5 : Abscissa of the point observed along the major axis.
Column 6 : HI flux at the point of abscissa x_0.
Column 7 : Half width of the beam at $1/e$ of the central value (in arcmin).
Column 8 : HI radius corresponding to the point where the model HI surface density has fallen to $1/e$ of its central value.
Column 9 : HI radius finally adopted.
Column 10 : Diameter of the disk containing 50 % of the HI mass of the galaxy.
Column 11 : Diameter of disk containing 70 % of the HI mass of the galaxy.
Column 12 : Ratio of the 50 % HI diameter to the RC2 corrected optical one.
Column 13 : Total HI flux emitted by the galaxy.

(*) Excluding the high velocity feature observed at the point E 3.3 (see the corresponding discussion for this galaxy).

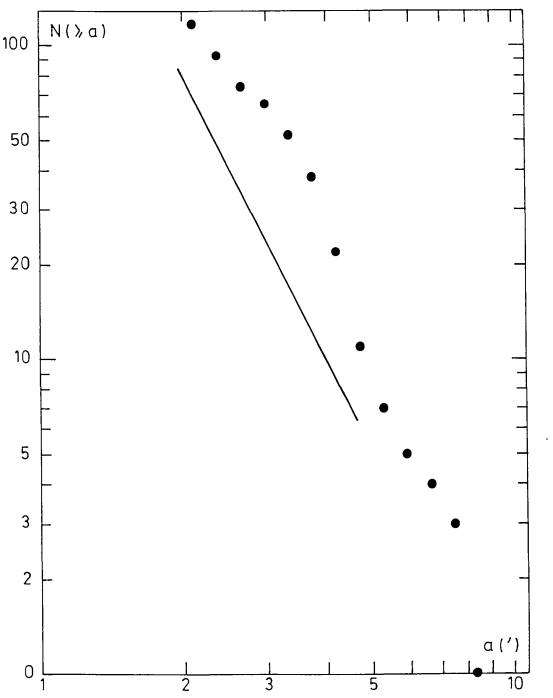

FIGURE 1. — Plot of the number of RC2 S0 galaxies with a declination in the range $(-1°, +38°)$ and having an apparent D_{25} diameter higher than a, as a function of a. If the S0's have an homogeneous space distribution and if the RC2 is complete, one expects for the curve a straight line parallel to the one drawn (slope -3).

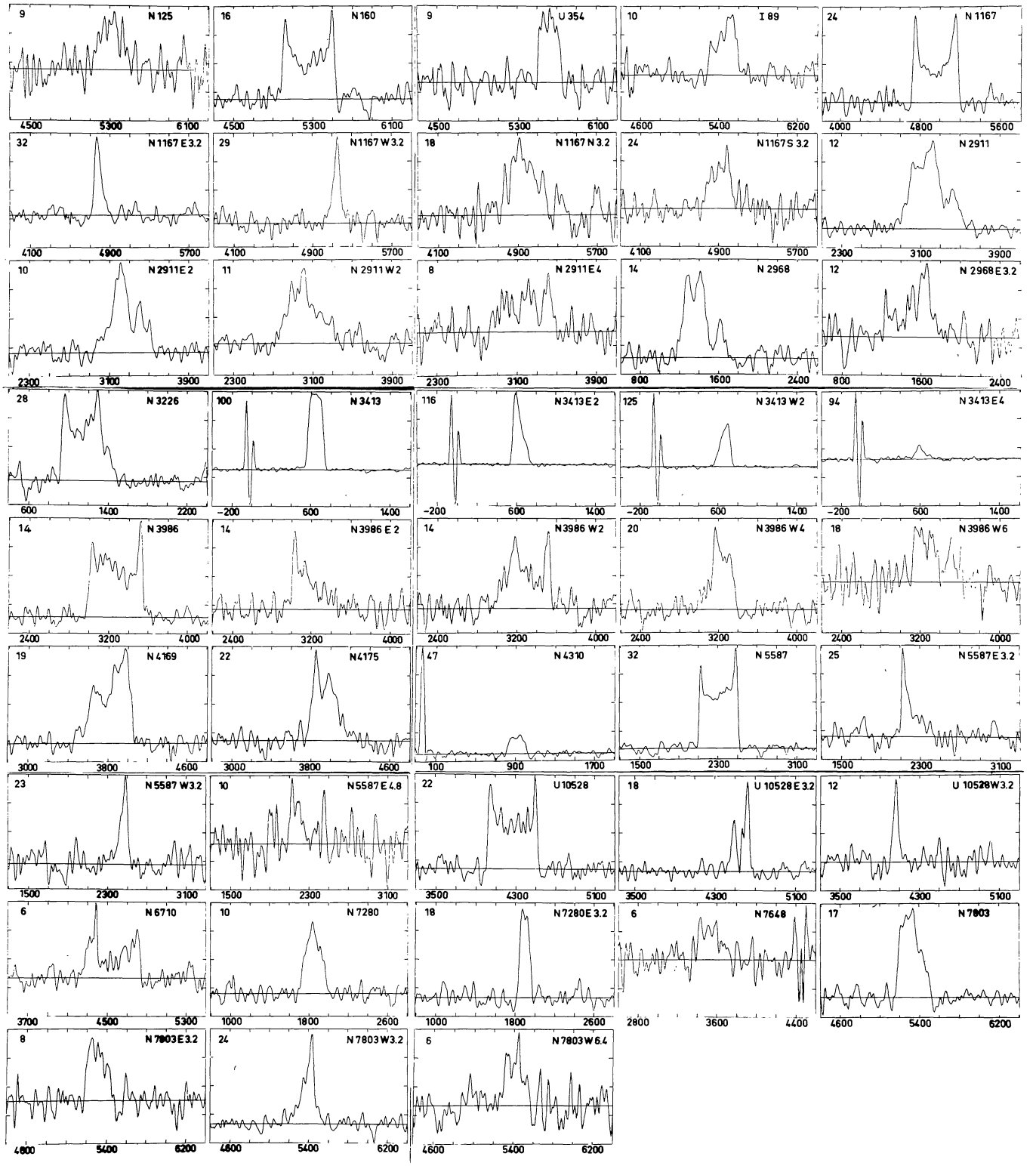

FIGURE 2. — HI profiles of the detected program-galaxies. Heliocentric velocities in the optical convention are in km s^{-1}. The number in the upper left corner represents the total range of the ordinates in mJy. For mapped galaxies, the number of the object is followed by the identification of the observed point (see text) ; (read 3.3 instead of 3.2, N1167 e3.3 instead of N1167 S3.2, and N7803 W7.3 instead of N7803 W6.6).

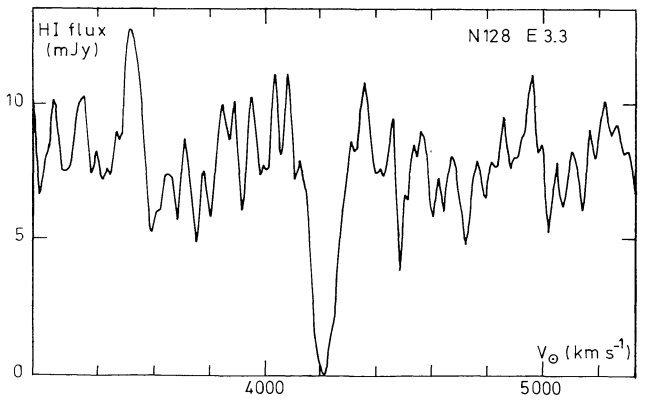

FIGURE 3. — Profile obtained at the position N128 E3.3. Abscissae in km s^{-1} (heliocentric velocities), ordinates in mJy.

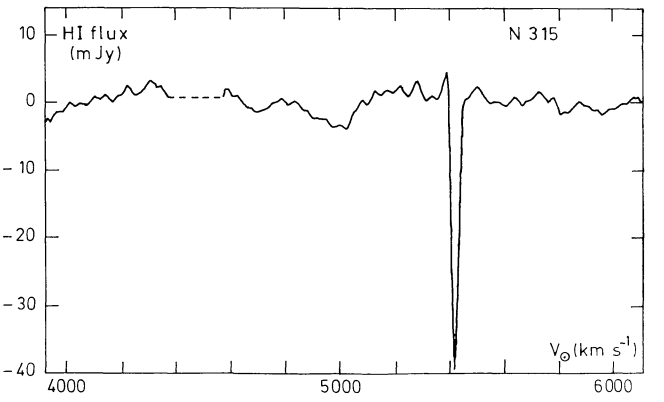

FIGURE 4. — Absorption lines in NGC 315. Abscissae in km s^{-1}, ordinates in mJy.

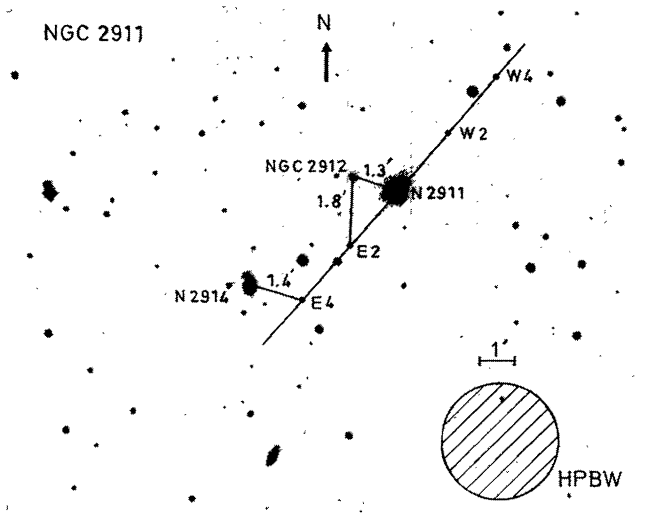

FIGURE 5.

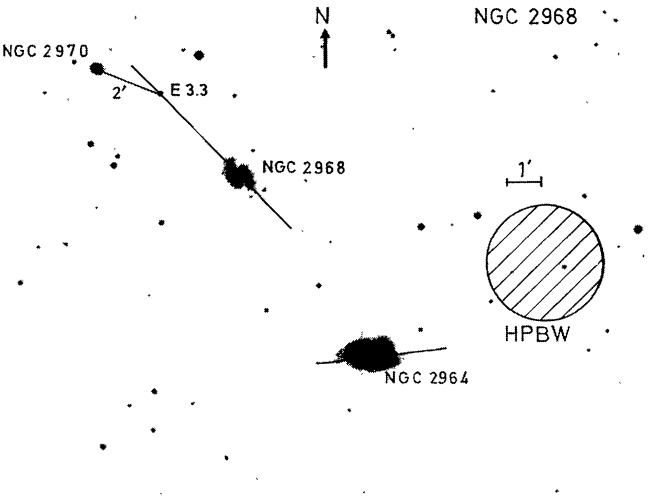

FIGURE 6.

FIGURES 5, 6, 7, 8, 10, 11. — Enlargements by a factor of 8 from the PSS blue prints for the galaxies having nearby confusing objects N2911, N2968, N3986, N4169-4175, N7280, N7803 respectively. North is upward ; the scale, the Arecibo HPBW at 21-cm and the different points observed in the mapping are indicated. In the figure 8, the 3 positions observed by Sulentic and Arp (1983) are noted by crosses.

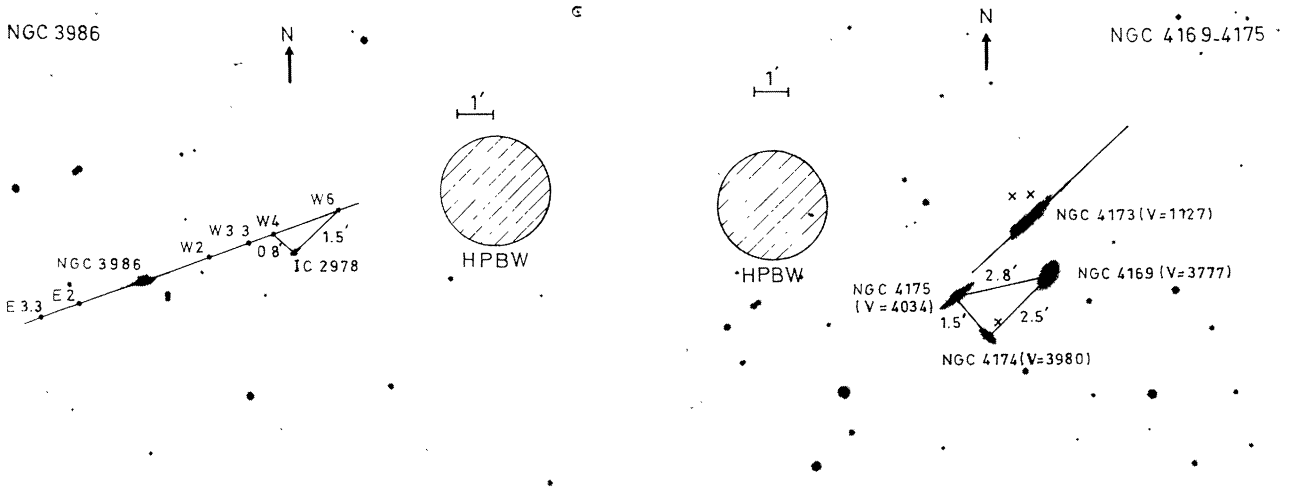

FIGURES 7 and 8 (see caption of figures 5 and 6).

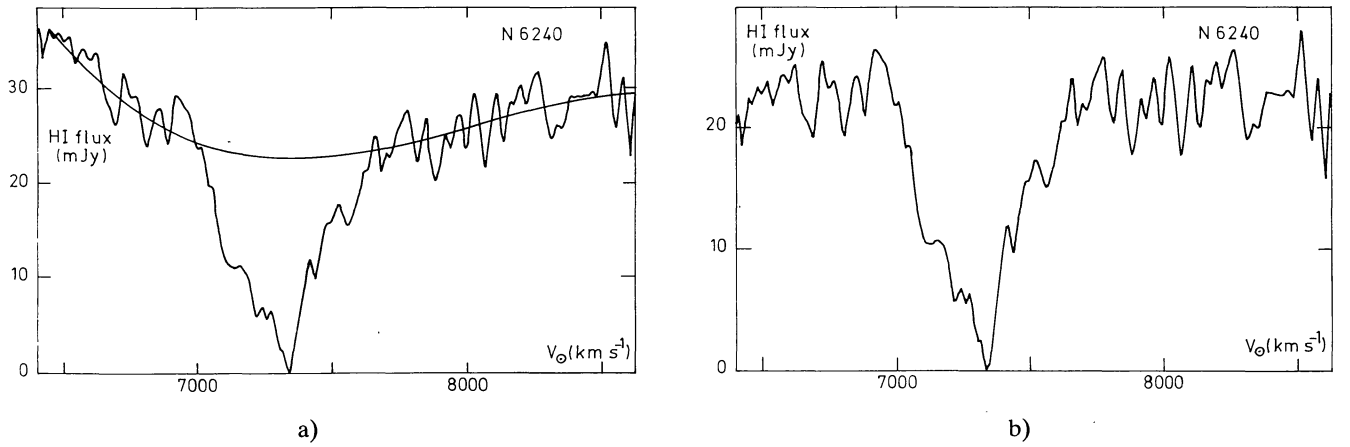

FIGURES 9(a) and 9(b). — Absorption profile obtained for NGC 6240 ; (a) without treatment ; (b) after subtraction of the baseline shown in (a). Abscissae in km s^{-1}, ordinates in mJy.

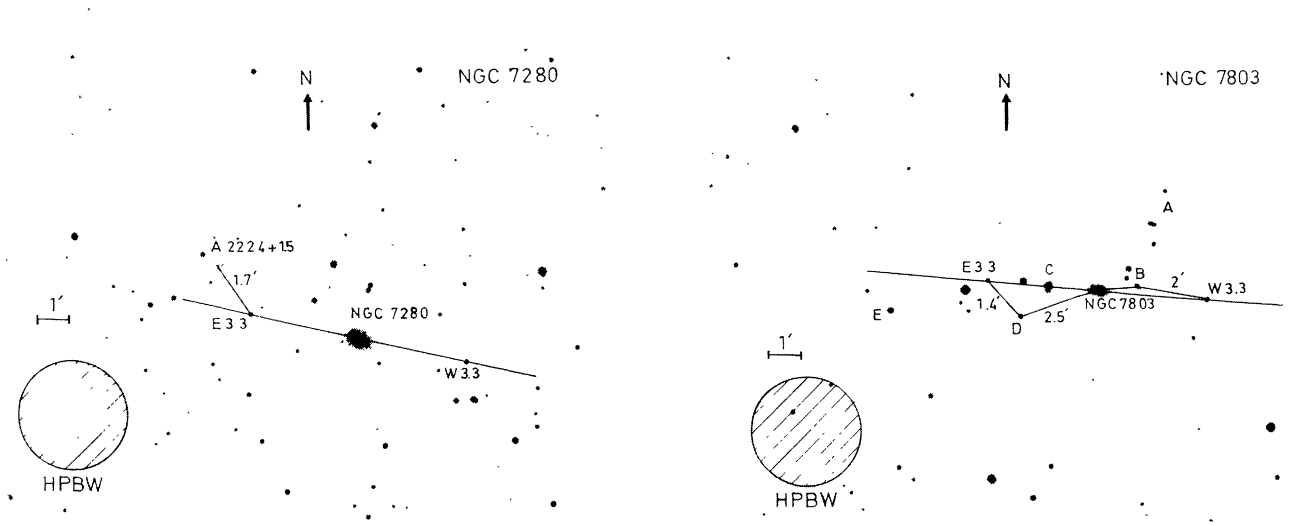

FIGURES 10 and 11 (see caption of figures 5 and 6).